Culture-independent characterization of a novel magnetotactic member affiliated to the Beta class of the Proteobacteria phylum from an acidic lagoon

Fernanda Abreu, Pedro Leão, Gabriele Vargas, Jefferson Cypriano, Viviane Figueiredo, Alex Enrich Prast, Dennis A. Bazylinski and Ulysses Lins

Abreu, F., Leão, P., Vargas, G., Cypriano, J., Figueiredo, V., Enrich Prast, A., Bazylinski, D. A., Lins, U., (2018), Culture-independent characterization of a novel magnetotactic member affiliated to the Beta class of the Proteobacteria phylum from an acidic lagoon, *Environmental Microbiology*, 20(7), 2615-2624. https://doi.org/10.1111/1462-2920.14286

Original publication available at:
https://doi.org/10.1111/1462-2920.14286

Culture-independent characterization of a novel, uncultivated magnetotactic member of the *Betaproteobacteria* class of the *Proteobacteria* phylum from an acidic lagoon

Fernanda Abreu[1§], Pedro Leão[1], Gabriele Vargas[1], Jefferson Cypriano[1], Viviane Figueiredo[2], Alex Enrich-Prast[2,3], Dennis A. Bazylinski[4] and Ulysses Lins[1]

[1]Instituto de Microbiologia Paulo de Góes, Universidade Federal do Rio de Janeiro, 21941-902, Rio de Janeiro, RJ, Brazil.

[2]Instituto de Biologia, Departamento de Botânica, Universidade Federal do Rio de Janeiro, 21941-902, Rio de Janeiro, RJ, Brazil.

[3]Department of Environmental Change, Linköping University, 58183, Linköping, Sweden.

[4]School of Life Sciences, University of Nevada at Las Vegas, Las Vegas, Nevada 89154-4004, USA.

[§]Corresponding author: Fernanda Abreu. Avenida Carlos Chagas Filho, 373; Centro de Ciências da Saúde; Instituto de Microbiologia; UFRJ; 21941-902; Rio de Janeiro, RJ, Brazil. E-mail: fernandaaabreu@micro.ufrj.br; Tel: +55-21-2560-8344 ext. 170; Fax: +55-21-2560-8028

Running head: Magnetotactic bacteria from *Betaproteobacteria* class

Conflict of Interest Statement: The authors declare no conflict of interest.

Originality Significance Statement

Magnetotactic bacteria are widely distributed in aquatic environments and are phylogenetically diverse with representatives in several different phyla. These bacteria are common members of microbial communities in most mesothermal environments with pH values around neutrality. However, uncultured alkaliphilic, moderately thermophilic, halophilic or strongly halotolerant, and psychrophilic magnetotactic bacteria have also been described in extreme environments across the globe. Here we report the presence of magnetotactic bacteria in sediments of a permanently acidic freshwater lagoon, which includes the first description of a magnetotactic bacterium belonging to the *Betaproteobacteria* class of the *Proteobacteria* phylum.

Summary

Magnetotactic bacteria (MTB) comprise a group of motile microorganisms common in most mesothermal aquatic habitats with pH values around neutrality. However, during the last two decades, a number of MTB from extreme environments have been characterized including: cultured alkaliphilic strains belonging to the *Deltaproteobacteria* class of the *Proteobacteria* phylum; uncultured moderately thermophilic strains belonging to the *Nitrospirae* phylum; cultured and uncultured moderately halophilic or strongly halotolerant bacteria affiliated with the *Delta-* and *Gammaproteobacteria* classes and an uncultured psychrophilic species belonging to the *Alphaproteobacteria* class. Here we used culture-independent techniques to characterize MTB from an acidic freshwater lagoon in Brazil (pH ~4.4). MTB morphotypes found in this acidic lagoon included cocci, rods, spirilla and vibrioid cells. Magnetite (Fe_3O_4) was the only mineral identified in magnetosomes of these MTB while magnetite magnetosome crystal morphologies within the different MTB cells included cuboctahedral (present in spirilla), elongated prismatic (present in cocci and vibrios) and bullet-shaped (present in rod-shaped cells). Intracellular pH measurements using fluorescent dyes showed that the cytoplasmic pH was close to neutral in most MTB cells and acidic in some intracellular granules. Based on 16S rRNA gene phylogenetic analyses, some of the retrieved gene sequences belonged to the genus *Herbaspirillum* within the *Betaproteobacteria* class of the *Proteobacteria* phylum. Fluorescent *in situ* hybridization using a *Herbaspirillum*-specific probe hybridized with vibrioid MTB in magnetically-enriched samples. Transmission electron microscopy of the *Herbaspirillum*-like MTB revealed the presence of many intracellular granules and a single chain of elongated prismatic magnetite magnetosomes. Diverse populations of MTB have not seemed to have been described in detail in an acid environment. In addition, this is the first report of an MTB phylogenetically affiliated with *Betaproteobacteria* class.

Introduction

Magnetotactic bacteria (MTB) biomineralize intracellular, membrane-bounded magnetite (Fe_3O_4) or greigite (Fe_3S_4) magnetic nanocrystals called magnetosomes (Bazylinski and Frankel, 2004). Magnetosomes are prokaryotic organelles used as part of a navigation system to more efficiently locate and maintain an optimal position in chemically-stratified aquatic environments for survival and growth (Cornejo et al., 2014).

MTB are ubiquitous in aquatic environments, being more commonly observed in sediments, but have also been described in wet soils (Fassbinder et al., 1990) and in the water columns of chemically-stratified habitats (Spring and Bazylinski, 2006). MTB were first reported in freshwater, brackish or marine environments with pH values close to neutrality and temperatures close to ambient (Bazylinski and Frankel, 2004). Mesophilic MTB include cultured species belonging to the *Alpha-*, *Delta-* and *Gammaproteobacteria* classes within the *Proteobacteria* phylum and several uncultured bacteria phylogenetically affiliated with the *Proteobacteria* and *Nitrospirae* phyla, and candidate phylum "*Omnitrophica*" (formerly OP3) (Lefèvre and Bazylinski, 2013). MTB signature genes in metagenomic sequences obtained from Sakinaw Lake (Canada), a lake where the pH varies from 5.7 to 6.5 and the temperature ranges from 8 to 19^{o}C (Perry, 1990), strongly indicate the possibility of a novel greigite-producing MTB belonging to the candidate phylum "*Latescibacteria*" (formerly WS3) (Lin and Pan, 2015) although an MTB of this type was not physically observed from the lake.

In the last two decades, a number of extremophilic MTB have been described and include halophilic, alkaliphilic, psychrophilic and thermophilic representatives (Bazylinski and Lefèvre, 2013). Some examples of these extremophiles include *Candidatus* Magnetoglobus multicellularis, an uncultured, slightly halophilic magnetotactic multicellular prokaryote (MMP) that inhabits a hypersaline lagoon in Brazil (Abreu et al., 2007). Strain SS-5, a rod-shaped, as yet unnamed MTB of the *Gammaproteobacteria*, capable of producing elongated

prismatic magnetite crystals in their magnetosomes, was isolated and grown in axenic culture from mud and water collected from the hypersaline Salton Sea in California (Lefèvre et al., 2012). Other somewhat halophilic MTB also include three cultured, alkaliphilic, apparently magnetotactic strains of *Desulfonatronum thiodismutans* that biomineralize bullet-shaped magnetite crystals in their magnetosomes (Lefèvre et al., 2011). These MTB, which are phylogenetically affiliated with the *Deltaproteobacteria*, include: strain ML-1, isolated from water and sediment collected from Mono Lake, California; strain ZZ-1, isolated from water and sediment collected from Soda Spring, California; and strain AV-1, isolated from water and sediment collected from an unnamed, temporary pond in the Armagosa Valley, California (Lefèvre et al., 2011). These strains grow optimally at pH 9.0–9.5, but not at pH 8.0 (Lefèvre et al., 2011). An uncultured moderately thermophilic MTB from the *Nitrospirae* phylum was discovered in hot spring sediments collected from Great Boiling Springs, Nevada (Lefèvre et al., 2010). This vibrioid bacterium, tentatively named *Candidatus* Thermomagnetovibrio paiutensis, is most closely related to the non-magnetotactic bacterium *Thermodesulfovibrio hydrogeniphilus,* which also inhabits hot springs and is distantly related to other MTB within the *Nitrospirae* phylum (Lefèvre et al., 2010). Finally, uncultured, psychrophilic MTB belonging to the *Alphaproteobacteria* have been described from marine sediments in Antarctica (Abreu et al., 2016). Although MTB were recently reported as being present in natural acid mine drainage biofilms (Goltsman et al., 2015), diverse populations of MTB have apparently not been found and/or reported from acidic environments.

Phylogenetic analyses based on 16S rRNA gene sequences from cultured and uncultured MTB show clearly that MTB are phylogenetically spread widely within the *Bacteria* domain (Lefèvre and Bazylinski, 2013). However, the phylogenetic diversity of MTB may be significantly underestimated because: 1) relatively few species have been isolated and grown in pure culture; 2) the phylogenetic affiliation of uncultured MTB requires light microscopy to

confirm the magnetotactic behavior, identification of the magnetosome mineral phase and phylogenetic identification, all of which must be linked; and 3) in some habitats, numbers or abundance of a specific morphotype or species of MTB might be very low. Here, we used culture-independent techniques to characterize MTB from an acidic freshwater lagoon in Brazil. Based on cell and magnetosome composition and morphology, several MTB morphotypes were identified, including rods, spirilla, vibrios and cocci. Notably, phylogenetic analyses and fluorescent *in situ* hybridization (FISH) indicate the presence of a novel species of MTB belonging to the *Betaproteobacteria* class.

Results

Sampling site

Comprida Lagoon is a tropical coastal lagoon in the South Hemisphere (Alves-de-Souza et al., 2006). This lagoon is shallow with regard to average depth and contains brown-colored, freshwater with an average pH of 4.9 and high concentrations of humic compounds (probably responsible for the brown coloring of the water), high average concentrations of dissolved organic carbon and dissolved nitrogen (Branco et al., 2000). During the entire sampling period, the pH of the lagoon water was consistently ~4.4. Vertical distribution of MTB along a sediment profile showed that they mainly inhabited the oxic-anoxic interface (OAI) at XX cm depth (Figure 1 A), indicating that these MTB have a XXXX respiratory metabolism. The pH in this sediment region containing MTB was 4.9.

Light and electron microscopy of MTB collected from the Comprida Lagoon

Light microscopy observations of magnetically-enriched (Lins et al., 2003) sediment and water samples taken from at or near the OAI of the Comprida Lagoon showed a relatively

strong diversity of MTB. Cell morphotypes included rods, cocci, spirilla and vibrioid cells (Figure 1 B). The vibrioid-shaped MTB each contained two conspicuous intracellular granules and were very abundant compared to other MTB morphotypes, corresponding to approximately 82% of the total MTB observed after magnetic-enrichment of the sample. (Figure 1 B, black arrowheads). Cells of this vibrioid morphotype were, on average (n = 32), 4.1 ± 0.8 μm in length and 2.1 ± 0.4 μm in width, and were often clustered in linear chains at the edge of the drop when observed using the hanging drop assay (Frankel et al., 1997). All MTB observed exhibited south-seeking magnetotactic behavior.

Ultrastructural analysis of MTB from magnetically-enriched samples by transmission electron microscopy (TEM) showed that the shape and size of magnetosomes varied among MTB morphotypes (Fig. S1). Although the composition of every type of magnetosome crystal was not determined, crystal TEM characteristics were typical of magnetite and there were no characteristics of greigite (e.g., a less consistent crystal morphology and a "wrinkled" appearance on the crystal surface (Pósfai et al., 1998)). Magnetosome average length, width and shape factor for each morphotype is shown in Table S1. Rod-shaped cells with several granules contained bullet-shaped magnetosomes organized in multiple chains within the cell (Fig. S1A). The size and shape factor of these bullet-shaped crystals ranged from 45.9 to 114.2 nm and 0.28 to 0.74, respectively (Figs. S1B and S1C). Figure S1D shows a TEM image of a magnetotactic coccus with a single chain of elongated prismatic magnetosomes. The size and shape factor of these crystals ranged from 102.1 to 178.1 nm and 0.60 to 0.83, respectively (Figs. S1H and S1I). Cells of the spirillar morphotype contained cuboctahedral magnetosome crystals (Figure S1G) with crystal size and shape factors ranging from 27.0 to 70.9 nm and 0.68 to 0.94, respectively (Figs. S1H and S1I). Cells of the vibrioid morphotype (Fig. S1J) contained elongated prismatic magnetosome crystals organized in a single chain along the long axis of the cell and as well as conspicuous electron-dense granules. The size and shape factor of these

prismatic magnetosome crystals ranged from 27.3 to 100.9 nm and 0.34 to 0.88 (Figs. S1K and S1L), respectively.

Intracellular pH of MTB from the Comprida Lagoon

The intracellular pH of MTB inhabiting the acid environment of the Comprida Lagoon was determined using pH-sensitive fluorescent dyes, which show negligible fluorescence at neutral pH, but a clear and strong fluorescence signal under acidic conditions (Breeuwer, et al., 1996). When stained with this dye, cells of the spirilla and cocci showed no and a low fluorescence signal, respectively (Fig. 2A, inset). In contrast, the vibrioid cells showed an intense fluorescent signal, seemingly associated the cytoplasmic granules (Fig. 2B, inset). Cells of the large rod-shaped morphotype showed a very high fluorescent signal again seemingly associated with the numerous granules present in each cell (Fig. 2C, inset).

Phylogeny of the vibrioid morphotype

Whole cell PCR for 16S rRNA gene amplification and sequencing was performed on cells purified using magnetic separation techniques. Notably, one gene sequence retrieved from these cells (AN: MG310191), was 98-99% similar to uncultured and cultured species of the genus *Herbaspirillum* of the *Betaproteobacteria* class of the *Proteobacteria* phylum in the domain *Bacteria* (Fig. 3A). To confirm that the betaproteobacterial 16S rRNA sequence that we recovered belonged to the magnetotactic vibrioid morphotype, we used FISH using a *Herbaspirillum*-specific probe. Vibrioid-shaped cells each containing two intracellular granules, as described earlier, clearly hybridized to a universal *Bacteria*-specific probe and a *Herbaspirillum*-specific probe (Fig. 3B-E). This magnetotactic morphotype was referred to as strain CLV-1. The *Herbaspirillum*-specific probe signal did not hybridize with any cell type in magnetically-enriched samples of MTB, as shown in Figures 3C and 3D (arrowhead). These

other MTB morphotypes clearly hybridized the universal *Bacteria*-specific probes but not with the *Herbaspirillum*-specific probe. Together, the results from light and electron microscopy and FISH clearly link the vibrioid magnetotactic morphotype (Figs. 1B and S1J) to the uncultured strain CLV-1 and to a phylogenetic affiliation with *Betaproteobacteria* class of the *Proteobacteria* phylum. We did not obtain other 16S rRNA gene sequences from separated MTB from the Comprida Lagoon most probably due to the fact the predominant morphotype in separated MTB was the vibrioid morphotype.

Magnetosome characterization in strain CLV-1

Conventional TEM imaging of ultra-thin sections of magnetically-enriched samples showed that magnetosome crystals were enveloped by a membrane (Fig. 4B). High-resolution TEM (HRTEM) and energy-dispersive X-ray spectroscopy (EDS) microanalysis in scanning TEM (STEM) mode was performed specifically for the elongated prismatic magnetosome crystals found in cells of the vibrioid MTB. HRTEM imaging and fast Fourier transform (FFT) pattern of the magnetic crystals in magnetosomes were composed of magnetite (Fig. 4C). EDS elemental microanalysis and elemental mapping (Figs. 4D-G) showed the crystals were composed of iron (Fig. 4E) and oxygen (Fig. 4F). Sulfur was not observed in these crystals (Fig. 4G) also consistent with the iron oxide magnetite. STEM images showed crystalline defects around the borders of some magnetosomes (Fig. 5A). Three-dimensional modeling based on STEM tomography showed the relative spatial distribution of magnetosomes to be organized as a single chain positioned along the long axis of the cells (Fig. 5B).

Discussion

The presence of a relatively diverse population of MTB in an acidic aquatic environment suggests that those MTB are acid tolerant and perhaps even moderately acidophilic. The

discovery of MTB in a natural acid mine drainage biofilm (Goltsman et al., 2015) supports this contention. Based on the ability of MTB to concentrate iron from their local environment for magnetosome production, it seems is reasonable to assume that in an acidic aquatic system, where iron ions are more soluble, MTB play an important role in accumulating this element. Thus MTB may represent an important group of organisms in iron geochemical cycling in these environments.

It is well known that environmental/culture conditions influence the biomineralization of magnetosomes by MTB (Faivre et al., 2008; Moisescu et al., 2014). In particular, low pH appears to alter iron uptake by cultivated *Magnetospirillum* species as well as the morphology and magnetic properties of magnetosome magnetite crystals (Moisescu et al., 2014). For example, Moisescu et al. (2014) showed that cells of *M. gryphiswaldense* strain MSR-1 produced smaller, poorly crystalline superparamagnetic magnetosome magnetite crystals rather than their typical cuboctahedral crystals when grown at pH 6.0, while growth under neutral to slight alkaliphilic conditions resulted in the biomineralization of larger "normal" crystalline single domain magnetite magnetosome crystals. Interestingly, MTB found in the Comprida Lagoon possessed magnetosome magnetite crystals with well-defined crystal morphologies with sizes compatible with single domain magnetite crystals despite the low pH of the lagoon. The acidic pH in the lagoon therefore, apparently did not affect magnetosome magnetite formation by MTB there. Because the cytoplasmic pH in MTB collected from the acidic sediment was close to neutral in all MTB morphotypes (except for the intracellular granules produced by some MTB) as evidenced by the intracellular pH assay, these organisms likely have an efficient mechanism of maintaining the intracellular pH close to neutrality as do known acidophiles (Dopson et al., 2017).

Maybe the most important result of this work is the discovery of a MTB phylogenetically affiliated with the *Betaproteobacteria* class of the *Proteobacteria* phylum as no MTB of this

group has been described. This finding clearly expands the known phylogenetic diversity of the MTB in general although it also raises new insights and questions regarding the origina and evolution of magnetotaxis in prokaryotes, specifically in the domain *Bacteria*. Although using metagenomics to determine the suite of *mam* and other magnetosomes genes would provide more information to better investigate the evolution of magnetotaxis in the *Proteobacteria* in particular, our results do provide some interesting and important information. There is a consistent, strong correlation between magnetosome crystal composition and morphology and phylogenetic affiliation in MTB (reference). Moreover, this correlation has been used to construct a possible evolutionary path of magnetosome synthesis and magnetotaxis.

MTB of the earliest diverging phylogenetic groups of the domain *Bacteria* (i.e., Candidate phylum "*Omniotriphica*", *Nitrospirae* phylum, and the *Deltaproteobacteria* class) biomineralize bullet-shaped crystals of magnetite, with some species in the *Deltaproteobacteria* also synthesizing greigite (Lefèvre and Bazylinski, 2013). Later diverging groups, including the *Alpha-* and *Gammaproteobacteria* classes of the *Proteobacteria* phylum biomineralize only cuboctahedral and elongated prismatic crystals of magnetite in their magnetosomes (reference). The *Delta-* and *Epsilonproteobacteria* are thought to have branched off the *Proteobacteria* lineage prior to the divergence of the *Alpha-*, *Beta-* and *Gammaproteobacteria* (Lefèvre and Bazylinski, 2013). Given this evolutionary scenario, then it seems likely that any MTB of the *Betaproteobacteria* would biomineralize cuboctahedral and/or elongated prismatic crystals of magnetite as the mineral phase of their magnetosomes. Our results show clearly that the magnetotactic betaproteobacterium we describe here biomineralizes elongated prismatic magnetite crystals in their magnetosomes which is consistent with the evolutionary model presented above. According to this same premise and the preponderance of current evidence, the morphologies of magnetosome crystals in other morphotypes of MTB from the Comprida Lagoon might indicate or at least suggest, that the phylogenetic affiliations of these MTB. For

example, the bullet-shaped magnetite-producing rod in the lagoon is very likely affiliated with *Deltaproteobacteria* class of the *Proteobacteria* phylum, the *Nitrospirae* phylum or even the Candidate phylum "*Omnitrophica*" (Lefèvre and Bazylinski, 2013).

Based on magnetosome crystal dimensions and on STEM tomography results, it is reasonable to assume that magnetite magnetosome biomineralization in strain CLV-1 from the *Betaproteobacteria* also occurs along the <111> axis, which coincide with the axis of the arrangement of the magnetosome chain, as occurs for MTB within the *Proteobacteria* phylum (Pósfai et al., 2013). Interestingly, STEM tomography showed that some magnetosome magnetite crystals within the magnetotactic *Hebaspirillum* exhibited surface defects in the crystallographic structure. These defects are occasionally observed in cells of some cultured MTB grown under specific conditions (Moisescu et al., 2014) but not usually observed in magnetosome magnetite crystals of MTB cells collected from environmental samples. Because optimum growth of cultivated *Herbaspirillum* species occurs between pH 5.3-8.8 (Baldani et al., 2015), defects in the magnetite crystals we observed might be caused by the low environmental pH found in Comprida Lagoon as has been found for magnetosome magnetite imperfections in *Magnetospirillum gryphiswaldense* strain MSR-1 when grown under acidic conditions (Moisescu et al., 2014). Future metagenomic studies of MTB from Comprida Lagoon should provide important information regarding magnetosome biomineralization in acidic environments. In addition, genomic data from the magnetotactic betaproteobacterial strain CLV-1 should provide great insight into the diversity of MTB in general and the evolution of magnetotaxis.

Experimental Procedures

Sampling and magnetic enrichment

The sampling site was Comprida lagoon, a permanently acidic freshwater lagoon located close to the Atlantic Ocean at the Restinga de Jurubatiba National Park (22°16.723'S; 41°39.415'W), Rio de Janeiro State, Brazil. The average lagoon's water pH is 4.9 with a high concentration of humic compounds (Branco et al. 2000). Samples of water and sediment were collected using 1 liter plastic bottles in December 2013 and May 2015. At the time of sampling, pH was 4.4. Bottles were stored at room temperature in the laboratory under dim light for several weeks. The pH of the lagoon water was measured using a S20K Mettler Toledo pH meter (Mettler-Toledo International Inc., Columbus, USA). Magnetic enrichment was performed using a specially customized glass apparatus exposed to an artificial magnetic field for 15 minutes according to Lins et al. (2003).

Light and fluorescence microscopy

For MTB detection and morphological characterization, samples were observed using the hanging drop technique and imaged by Nomarski differential interference contrast (DIC) microscopy using a Zeiss Axioimager microscope (Carl Zeiss, Oberkochen, Germany) equipped with a fluorescence microscopy mode. The percentage of magnetotactic vibrioid cells was estimated by counting MTB morphotypes in random DIC images; A total of 826 MTB were counted. For intracellular pH measurement, the fluorescent kit containing pHrodo Green AM Intracellular pH Indicator dye and PowerLoad Concentrate (Life Technologies, Carlsbad, USA) was used according to the manufacturer's instructions and imaging was done using a Zeiss filter set 09 (Excitation: BP 450-490 nm; Beam splitter : FT 510 nm; Emission: LP 515 nm).

Transmission electron microscopy and tomography

For conventional transmission electron microscopy, magnetically enriched cells were deposited on formvar-coated 300 mesh copper grids, washed with distilled water and imaged using a FEI Morgagni (FEI Company, Eindhoven, The Netherlands) transmission electron

microscope at 80 kV. Magnetosome length, width, size ((length + width)/2) and shape factor (width/length) was determined by image analysis using the iTEM software suite (Olympus corporation, Tokyo, Japan). Magnetically enriched samples were fixed, dehydrated, embebded in resin and ultrathin sectioned as described in Leão et al. (2007). Sample sections were collected in 300 mesh copper grids, stained with uranyl acetate and lead citrate and imaged using a FEI Morgagni TEM in the same conditions described above. For high resolution transmission electron microscopy (HRTEM), cells were imaged using a Titan-FEG transmission electron microscope (FEI Company, Eindhoven, The Netherlands) operated at 200 kV and equipped with a 2k x 2k Gatan UltraScan 1000 CCD camera. Fast Fourier transform from HRTEM images were obtained using the Digital Micrograph software (Gatan, Inc, Pleasanton, USA). Energy dispersive X-ray spectroscopy (EDS) elemental mapping was done using an EDS system with four embedded SDD detectors in scanning transmission electron microscopy (STEM) mode to generate elemental maps of oxygen, iron and sulfur. Tomography data was obtained in STEM mode using a Tecnai G20 field emission gun microscope at 200 kV. Single tilt axis image series were acquired from +60° to -60° at 64,000x direct magnification with automatic correction for focus and image shift variations using TIA software. Images were recorded with a Fishione high-angle annular dark field (HAADF) detector model M3000. Reconstruction and alignment of STEM tilt series were conducted using the IMOD package.

Phylogenetic analysis based on the 16S rRNA coding gene

After magnetic enrichment and sample washing with filter sterilized and autoclaved lagoon water, samples were used in whole cell polymerase chain reaction (PCR) performed with DreamTaq Green PCR Master Mix (Thermo Scientific Inc., Waltham, USA) and universal 16S rRNA gene primers 27F (5`-AGAGTTTGATCMTGGCTCAG-3`) e 1492R (5`-TACGGHTACCTTGTTACGACTT-3`) (Lane, 1991). PCR products were cloned using

pGEM®-T Easy Vector System I (Promega, Madison, USA). Clones were sequenced by Macrogen Inc. (Seoul, South Korea). For phylogenetic analysis, retrieved sequences were aligned using ClustalW alignment tool in the BioEdit software (Hall, 1999). MEGA 6 software was used for phylogenetic tree construction (Tamura et al., 2013).

Fluorescent *in situ* hybridization

Based on the 16S rRNA coding gene sequences retrieved from environmental samples, a probe for *Herbaspirillum* genus (5´ - CAAGCTCCTATGCTGCCGTT- 3´; Sanguin et al., 2006) was used in fluorescent in situ hybridization (FISH) using 20% formamide according to Pernthaler et al. (2001).

Acknowledgements

We thank Dr. Luiz Henrique de Almeida from COPPE-UFRJ for HRTEM and analytical facilities, Dr. Marcos Paulo Figueiredo de Barros from NUPEM-MACAÉ, UFRJ, Dr. Lia C. R. S. Teixeira from Universidade Estadual do Rio de Janeiro and Dr. Ana Carolina Araújo from Universidade Federal de São Carlos for sampling. Microscopy Facilities: Centro Nacional de Bioimagem (CENABIO, UFRJ), Unidade de Microscopia Multiusuário Souto-Padrón and Lins (UniMicro, UFRJ). FA, PL, JC, and UL are supported by Brazilian agencies CNPq, CAPES and FAPERJ. DAB is supported by U.S. National Science Foundation (NSF) grant EAR-1423939.

References

Abreu, F., Martins, J.L., Silveira, T.S., Keim, C.N., Lins de Barros, H.G.P, Gueiros-Filho, F., and Lins, U. (2007) 'Candidatus Magnetoglobus multicellularis', a multicellular

magnetotactic prokaryote from a hypersaline environment. Int J Syst Bacteriol 57: 1318-1322.

Abreu, F., Araujo, A.C.V., Leão, P., Silva, K.T., Marques, F., Cunha, O., et al. (2016) Culture-independent characterization of novel psychrophilic magnetotactic cocci from Antarctic marine sediments. Environ Microbiol 18: 4426-4441.

Alves-de-Souza, C., Menezes, M., and Huszar, V. (2006) Phytoplankton species composition and morphological functional groups in a tropical humic coastal lagoon, Brazil. Acta Bot Bras 20:701-708.

Baldani, J. I., Baldani, V. L. D. and Döbereiner, J. 2015. Herbaspirillum. Bergey's Manual of Systematics of Archaea and Bacteria. 1–13.

Bazylinski, D.A., and Frankel, R.B. (2004) Magnetosome formation in prokaryotes. Nat Rev Microbiol 2: 217-230.

Bazylinski, D.A., and Lefèvre, C.T. (2013) Magnetotactic bacteria from extreme environments Life 3: 295-307.

Branco, C.W.C.; Esteves, F.A. and Kozlowsky-Suzuki, B. (2000) The zooplankton and other limnological features of a humic coastal lagoon (Lagoa Comprida, Macaé, RJ) in Brazil. Hydrobiologia 437: 71-81

Cornejo, E., Abreu, N., and Komeili, A. (2014) Compartmentalization and organelle formation in bacteria. Curr Opin Cell Biol 26:132-138.

Dopson, M., Holmes, D.S., Lazcano, M., McCredden, T.J., Bryan, C.G., Mulroney, K.T., Steuart, R., Jackaman, C. and Watkin, E.L.J. (2017) Multiple Osmotic Stress Responses in Acidihalobacter Prosperus Result in Tolerance to Chloride Ions. Front Microbiol 7, 2132. doi: 10.3389/fmicb.2016.02132

Breeuwer, P., Drocourt, J., Rombouts, F.M., and Abee T. (1996) A novel method for continuous determination of the intracellular pH in bacteria with the internally conjugated fluorescent probe 5 (and 6-)-carboxyfluorescein succinimidyl ester. Appl Environ Microbiol 62: 178-183.

Faivre, D., Menguy, N., Pósfai, M., and Schüler, D. (2008). Environmental parameters affect the physical properties of fast-growing magnetosomes. American Mineralogist, 93: 463-469

Fassbinder, J. W., Stanjekt, H., and Vali, H. (1990). Occurrence of magnetic bacteria in soil. Nature, 343: 161-16, doi:10.1038/343161a0.

Frankel, R.B., Bazylinski, D.A., Johnson, M.S. and Taylor, B.L. (1997) Magneto-aerotaxis in marine coccoid bacteria. Biophysical Journal, 73 : 994-1000.

Goltsman, D.S. A., Comolli, L.R., Thomas, B.C., and Banfield, J.F. (2015) Community transcriptomics reveals unexpected high microbial diversity in acidophilic biofilm communities. The ISME Journal 9: 1014-1023.

Hall, T.A. (1999) BioEdit: a user-friendly biological sequence alignment editor and analysis program for Windows 95/98/NY. Nucl Acids Symp Ser 41: 95-98.

Lane, D.J. 1991. 16S/23S rRNA sequencing, p 115-175. In Stackebrandt E, Goodfellow M (ed), Nucleic acid techniques in bacterial systematics. Wiley and Sons, Chichester, UK.

Leão, P., Chen, Y. R., Abreu, F., Wang, M., Zhang, W. J., Zhou, K., Xiao, T., Wu, LF and Lins, U. (2017) Ultrastructure of ellipsoidal magnetotactic multicellular prokaryotes depicts their complex assemblage and cellular polarity in the context of magnetotaxis. Environmental microbiology. Environ Microbiol 6: 2151-2163.

Lefèvre, C.T., and Bazylinski, D.A. (2013) Magnetotactic bacteria. Ecology, diversity, and evolution of magnetotactic bacteria. Microbiol Mol Biol Rev 77: 497-526.

Lefèvre, C.T., Viloria, N., Schmidt, M.L., Pósfai, M., Frankel, R.B. and Bazylisnki, D.A. (2012) Novel magnetite-producing magnetotactic bacteria belonging to the Gammaproteobacteria. ISME J 6: 440-450.

Lefèvre, C.T., Frankel, R.B., Pósfai, M., Prozorov, T., and Bazylinski, D.A. (2011) Isolation of obligately alkaliphilic magnetotactic bacteria from extremely alkaline environments. Environ Microbiol 13: 2342-2350.

Lefèvre, C.T., Abreu, F., Schmidt, M.L., Lins, U., Frankel, R.B., Hedlund, B.P., and Bazylinski, D.A. (2010) Moderately thermophilic magnetotactic bacteria from hot springs in Nevada. Appl Environ Microbiol 11: 3740-3743.

Lin, W., and Pan, Y.X. (2015) A putative greigite-type magnetosome gene cluster from the candidate phylum Latescibacteria. Environ Microbiol Rep 7:237-242.

Lins, U., Freitas, F., Keim, C.N., Lins de Barros, H.G.P, Esquivel, D.S.M., and Farina, M. (2003) Simple homemade apparatus for harvesting uncultured magnetotactic microorganisms. Braz J Microbiol 34: 111-116.

Moisescu, C., Ardelean, I. I., and Benning, L. G. (2014) The effect and role of environmental conditions on magnetosome synthesis. Frontiers in microbiology, 5. doi: 10.3389/fmicb.2014.00049

Pernthaler, J., Glöckner, F.O., Schönhuber, W., and Amann, R. (2001) Fluorescence in situ hybridization with rRNA-targeted oligonucleotide probes. In Methods in microbiology: marine microbiology, vol. 30, J. Paul (ed.), United Kingdom, London: Academic Press Ltd., pp. 207-226.

Perry, K. A. (1990). The chemical limnology of two meromictic lakes with emphasis on pyrite formation (Doctoral dissertation, University of British Columbia).

Pósfai, M., Buseck, P. R., Bazylinski, D. A. and Frankel, R. B. (1998) Iron sulfides from magnetotactic bacteria: structure, composition, and phase transitions. Am. Mineral., 83:1469-1481.

Pósfai, M., Lefèvre, C. T., Trubitsyn, D., Bazylinski, D. A., and Frankel, R. B. (2013) Phylogenetic significance of composition and crystal morphology of magnetosome minerals. Frontiers in microbiology, 4. doi: 10.3389/fmicb.2013.00344.

Sanguin, H., Herrera, A., Oger-Desfeux. C., Dechesne, A., Simonet, P., Navarro, E., et al. (2006) Development and validation of a prototype 16S rRNA-based taxonomic microarray for Alphaproteobacteria. Environ Microbiol 8: 289-307.

Spring, S. and Bazylinski, D.A. (2006) Magnetotactic bacteria. Prokaryotes 2, 842-862.

Tamura, K., Stecher, G., Peterson, D., Filipski, A., and Kumar, S. (2013) MEGA6: Molecular Evolutionary Genetics Analysis version 6.0. Mol Biol Evol 30: 2725-2729.

Uebe, R. and Schüler, D. (2016) Magnetosome biogenesis in magnetotactic bacteria Nat Rev Microbiol 14: 621-637, doi:10.1038/nrmicro.2016.99

Figures and Tables

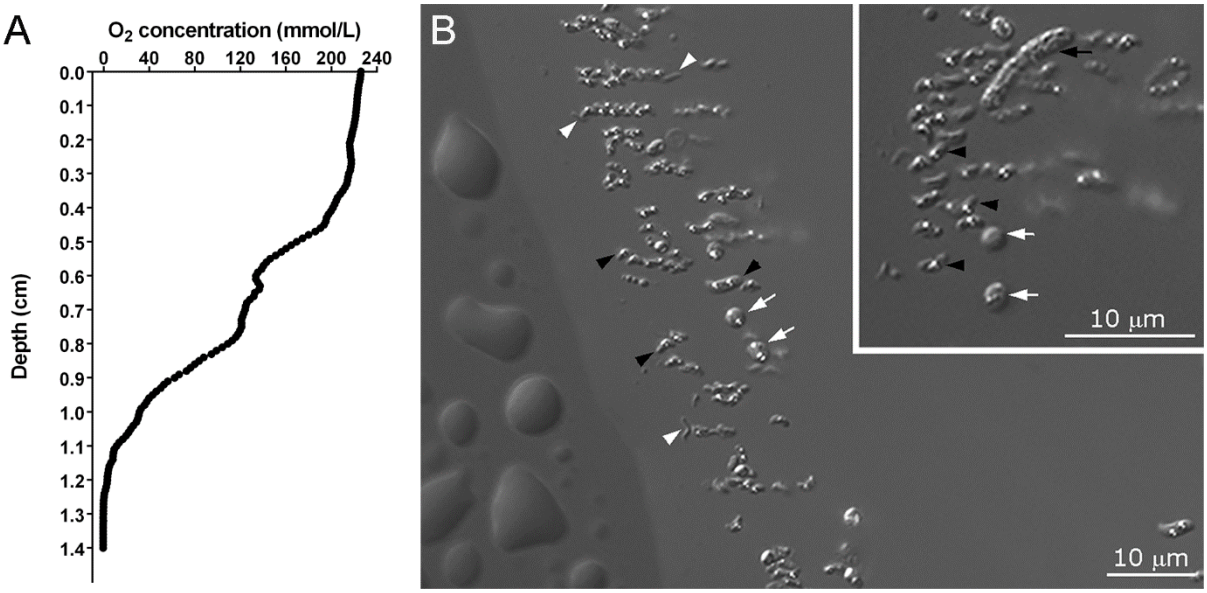

Fig. 1. Association of specific MTB morphotypes with sediment depth in the Comprida Lagoon. (A) Oxygen concentration [O_2] profile correlated with MTB distribution in sediment layers and water pH. (B) Differential interference contrast (DIC) microscopy image of MTB morphotypes present in magnetically-enriched samples from the Comprida Lagoon. Note the presence of vibrioid cells with cytoplasmic inclusions (black arrowheads), and cocci (white arrows), spirilla (white arrowheads) and a rod (inset, black arrow).

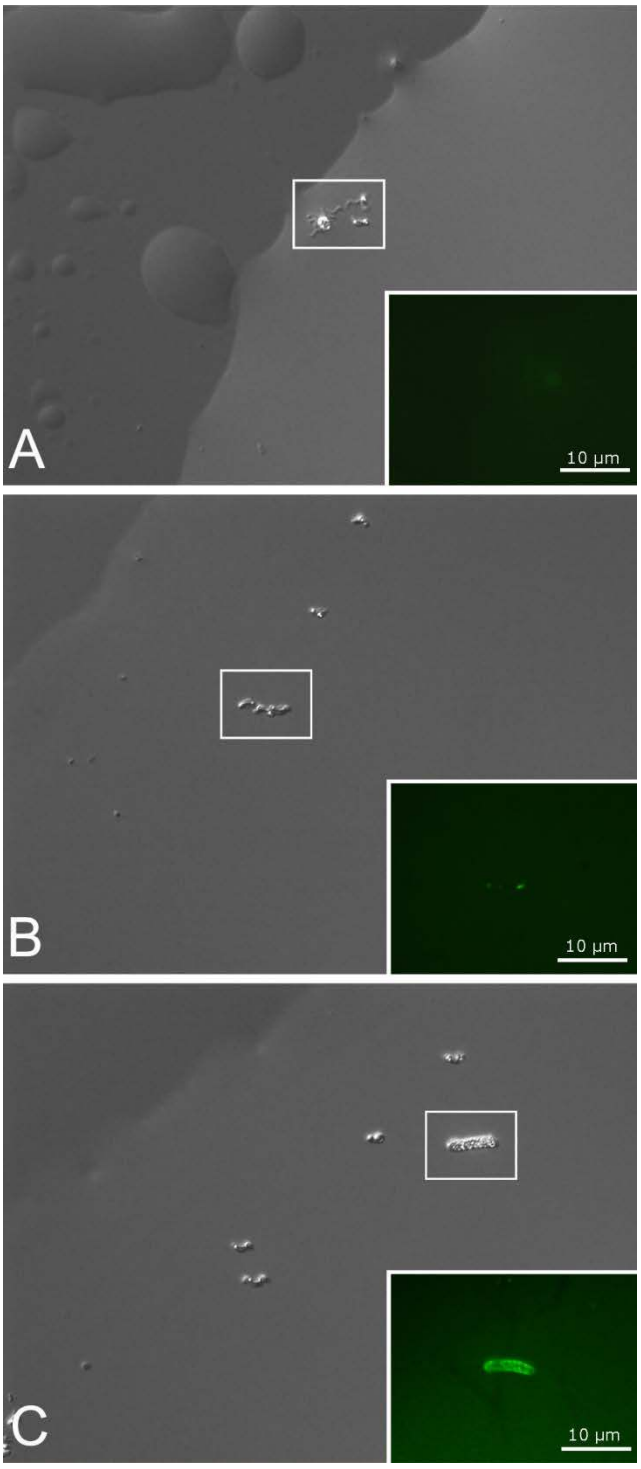

Fig. 2. Intracellular pH analysis of MTB using the fluorescent acid-sensitive dye pHrodo Green. (A) DIC microscopy images showing three MTB morphotypes from Comprida Lagoon: spirillar (helical), coccoid and vibrioid cells; (B) only vibrioid cells; (C) only rod-shaped cells. The inset in each image shows the fluorescent cell reaction of designated MTB corresponding to cells indicated by white squares in (A), (B) and (C), respectively, using fluorescence

microscopy. The fluorescence reactions indicate that the cytoplasm of the spirilla is neutral (absence of fluorescent signal) and a similar result for the coccus (low fluorescent signal). In contrast, the fluorescence reaction of the vibrioid cells (B) and the large rod-shaped bacteria (C) show a low intracellular pH, >6, in the region corresponding to the granule-like inclusions.

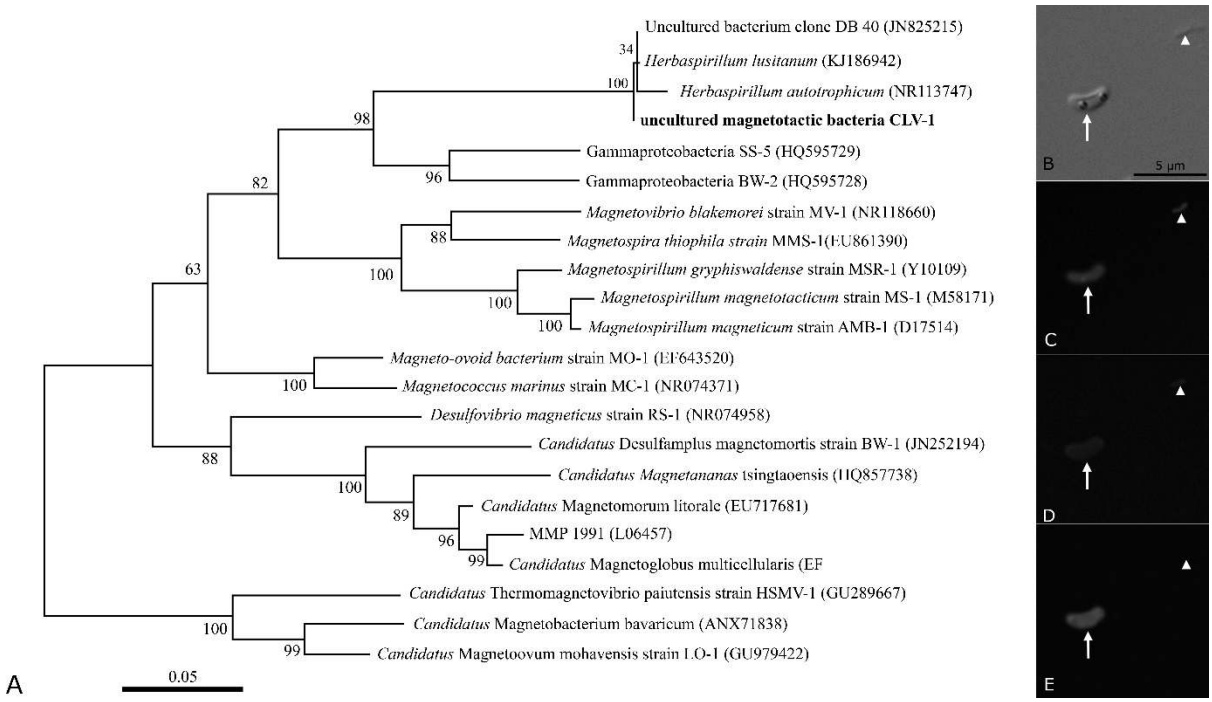

Fig. 3. Phylogenetic analysis and corresponding fluorescent *in situ* hybridization (FISH) of the MTB collected from the Comprida Lagoon belonging to the *Betaproteobacteria* class. (A) Maximum likelihood phylogenetic tree based on 16S rRNA gene sequences showing the position of the strain CLV-1 among other MTB and *Herbaspirillum* species. Bootstrap values were calculated for 1,000 replicates. GenBank accession numbers are given in parentheses. (B) DIC microscopy image of magnetic-enriched MTB, showing two cells; one containing a chain of magnetosomes and two intracellular granules (arrow) and another cell (arrowhead). (C) Fluorescence microscopy image of the same region shown in (B) stained with 4',6-diamidino-2-phenylindole (DAPI). Note that all cells stain with DAPI (arrow and arrowhead). (D) Fluorescence microscopy image of the same cells hybridized with the *Bacteria*-specific probes. Note the fluorescent signal on both cells (arrow and arrowhead). (E) Fluorescence microscopy image of the same cells hybridized with the *Herbaspirillum*-specific probe. The vibrioid-shaped cell with two granules hybridized to this specific probe (arrow) but not the other cell. COLOCAR AN e VER AN do MMP.

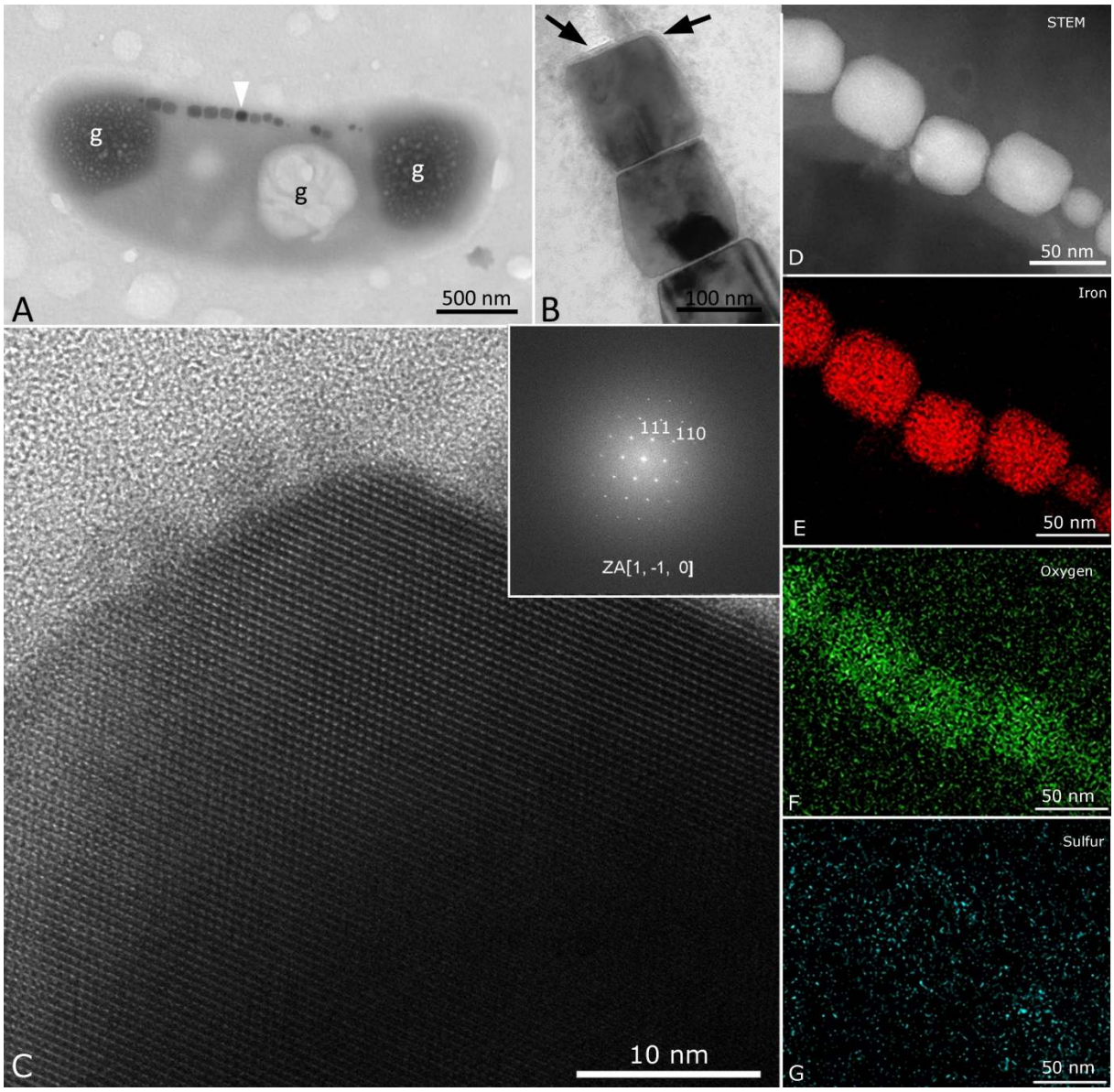

Fig. 4. Characterization of magnetosomes in strain CLV-1. (A) TEM image of a cell of the vibrioid MTB (strain CLV-1) Comprida Lagoon, showing the presence of an intracellular single chain of elongated prismatic magnetosomes as well a number of granule-like inclusions. (B) TEM image of an ultrathin section of a cell of strain CLV-1 showing that magnetosomes are enveloped by an electron-dense membrane (arrows). (C) High resolution TEM (HRTEM) image of a single magnetosome from strain CLV-1. Inset: fast Fourier transform (FFT) image corresponding to the [1,-1,0] zone axis of magnetite (Fe_3O_4). (D) High-angle annular dark-field (HAADF) image of a cell of strain CLV-1 showing a chain of magnetosomes with

corresponding elemental maps of iron (E); oxygen (F); and sulfur (G) of the magnetosome chain shown in (D).

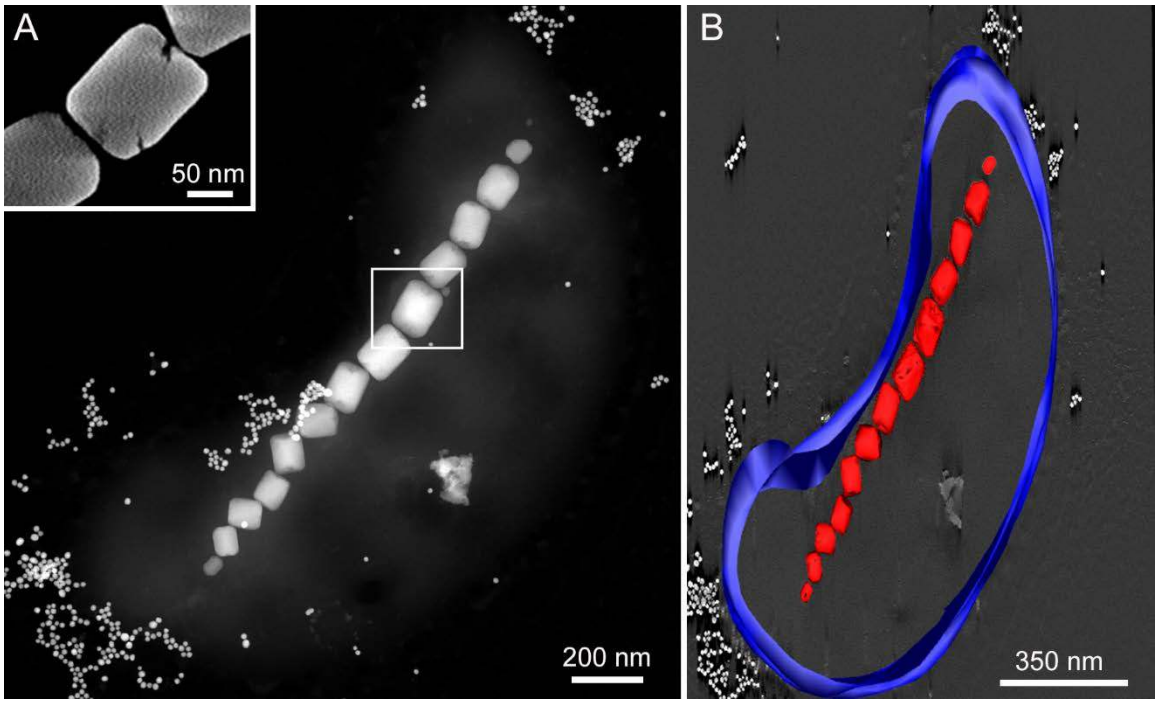

Fig. 5. Characterization of magnetosomes by electron microscopy. (A) Scanning TEM (STEM) image a magnetosome chain in a cell of CLV-1. Inset: Higher magnification of the region indicated by the white square in (A). Note the defects around the magnetosome magnetite crystal. (B) Three-dimensional reconstruction based on STEM tomography showing the relative spatial distribution of magnetosomes organized as a single chain within the cell.

Table S1. Magnetotactic bacteria (MTB) morphotypes found in the Comprida Lagoon and statistical data on size and shape factor of magnetosome crystals in these MTB.

Bacterial Morphotype	Cytoplasmic inclusions	Magnetosome habit	Size (nm)	Length (nm)	Width (nm)	Shape factor
Rod	several small	bullet-shaped	68.2 ± 13.5	42.6 ± 5.6	83.2 ± 23.0	0.53 ± 0.09
Coccus	one large	prismatic	144.8 ± 20.2	164.0 ± 25.8	120.9 ± 18.1	0.74 ± 0.05
Spirillum	several	cuboctahedra	51.7 ± 10.5	56.2 ± 11.8	47.3 ± 9.4	0.84 ± 0.05
Vibrioid	two large	prismatic	63.7 ± 16.9	78.1 ± 17.8	49.3 ± 18.9	0.63 ± 0.17

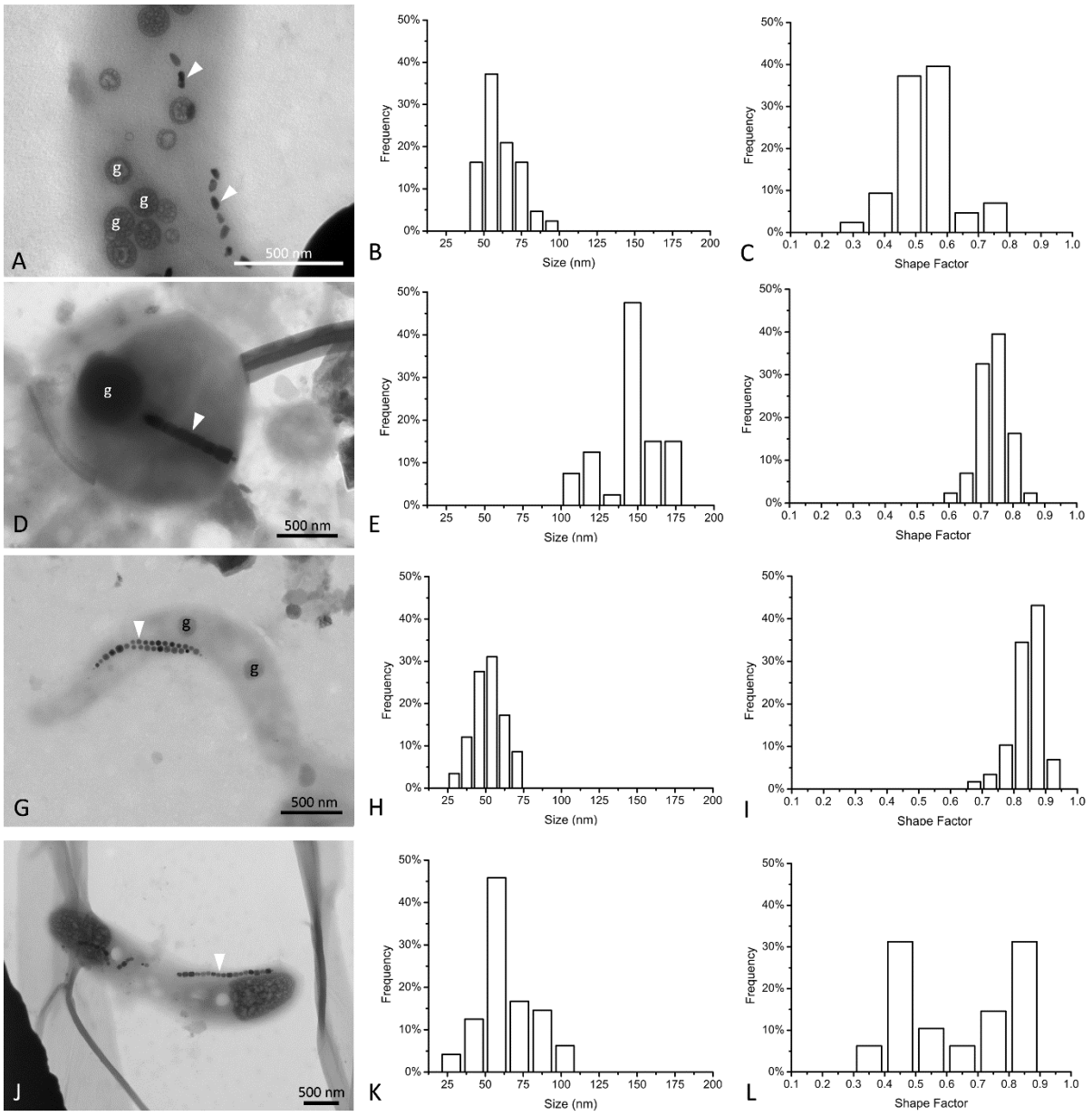

Fig. S1. Ultrastructure and magnetosome crystals morphologies in MTB from the Comprida Lagoon sediment. (A) Rod-shaped cell containing bullet-shaped magnetosomes (arrowheads). Size (B) and shape factor (C) distribution of magnetosome crystals shown in (A). (D) Magnetotactic coccus containing elongated prismatic magnetosomes (arrowhead). Size (E) and shape factor (F) distribution of magnetosome crystals shown in (D). (G) Magnetotactic spirillum containing cuboctahedral magnetosomes (arrowheads). Size (H) and shape factor (I) distribution of magnetosome crystals shown in (G). (J) Vibrioid cell (strain CLV-1) containing elongated prismatic magnetosomes (arrowhead) as well as two electron-dense and one electron-

lucent granules (g). Size (K) and shape factor (L) distribution of magnetosome crystals shown in (J).